

Corrosion Protection of Mild Steel by Applying TiO₂ Nanoparticle Coating via Sol-Gel Method¹

A. Shanaghi, A. R. Sabour, T. Shahrabi, and M. Aliofkhazraee

Surface Engineering Laboratory, Materials Engineering Department, Faculty of Engineering, Iran, Tehran, Tarbiat Modares University, P.O. Box: 14115–143

e-mail: sabour02@yahoo.com

Received November 2, 2007

Abstract—TiO₂ nanoparticle coatings possess good thermal and electrical properties and they are resistant to oxidation, corrosion, erosion and wear in high temperature environments. This property is very important factor in the applications such as pipelines, castings and automotive industry. In this investigation a uniform TiO₂ nanoparticle coating has been applied on mild steel, using sol-gel method. The coating was deposited on mild steel substrate by dip coating technique. The morphology and structure of the coating were analyzed using SEM, AFM and X-ray diffraction. The anticorrosion performances of the coating have been evaluated by using electrochemical techniques. It is worthy to note that the film uniformity was retained in high temperatures and no crack and flaking off from the substrate was observed. The Tafel polarization measurements provide an explanation to the increased resistance of TiO₂ nanoparticle coated mild steel against corrosion and i_{corr} was decreased from 18.621 to 0.174 $\mu\text{A}/\text{cm}^2$.

PACS numbers:

DOI: 10.1134/S2070205109030071

1. INTRODUCTION

Nanostructured TiO₂ thin films use in a wide range of applications. These applications consist of ultraviolet filters for optics and packing materials [1, 2], antireflection coatings for photovoltaic cells and passive solar collectors [3], photo catalysts for purification and treatment of water and air [4, 5], anodes for ion batteries [6], electrochromic displays [7], transparent conductors, self-cleaning coatings of windows and tiles [8], humidity sensors [9], gas sensors [10] and barrier layer for corrosion protection [11]. It has been shown that some applications greatly benefited from a nanostructured phase for TiO₂. Indeed production of nanostructured TiO₂ thin films has been recently carried out by several methods [12–14]. Several techniques have been used for the preparation of transparent TiO₂ thin films, which include sputtering [15] chemical vapour deposition [16, 17], pulsed laser deposition [18], laser molecular-beam epitaxy method [19], and sol-gel technique [20, 21]. The sol-gel technique has distinct advantages over the other techniques due to excellent compositional control, homogeneity on the molecular level due to the mixing of liquid precursors, and lower crystallization temperature. Moreover, the microstructure of the film deposited, i.e. the pore size, pore volume and surface area, by the sol-gel process can be tailored by the control of process variables [22] and a more generic approach to enhance corrosion resistance is to apply

protective films or coatings without crack. The presence of cracks and defects in coating, with increasing current density, will lead to localized corrosion [23].

Recently, sol-gel based alumina coating has been developed and characterized on stainless steel and mild steel substrate to improve its abrasion and corrosion resistance properties [24, 25]. Due to many applications of mild steel in industry, this work shows an attempt to increase the corrosion resistance properties of mild steel substrate by applying TiO₂ nanoparticle coating using the sol-gel method. Structural and micro-structural characterizations of thin films have been realized by X-ray diffraction (XRD), scanning electron microscopy (SEM) and atomic force microscopy (AFM). The Tafel polarization curves were employed to measure anticorrosion performance of the TiO₂ coatings in 3.5% NaCl solution and to discuss the mechanism of corrosion resistance for the coatings.

2. EXPERIMENTAL

The reagents were used in as received conditions. Since the water content of the sol has a critical role in the hydrolysis and polycondensation reactions, absolute ethanol (Merck 99%) was used as the solvent, ethyl acetoacetat (EAcAc) (Merck 99%) used as chelating agent, tetra n-butyl orthotitanate (TBT) (Merck 98%) was used as the precursor. TiO₂ sol was prepared from tetra-n-butyl titanate (TBT), ethanol, ethyl acetoacetate (EAcAc) and distilled water were mixed at room tem-

¹ The article is published in the original.

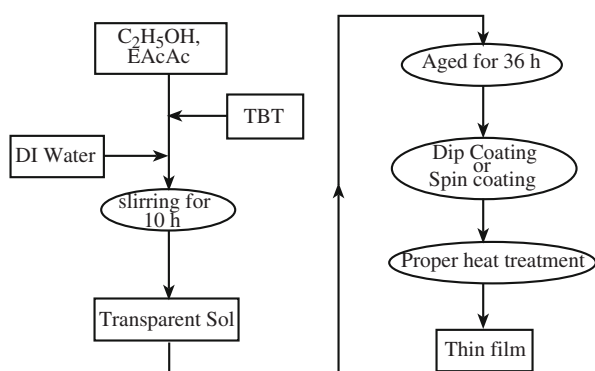


Fig. 1. Schematic preparation diagram for sol-gel derived TiO_2 nanoparticle.

perature following Fig. 1. In the experiment, the hydrolysis reaction was carried out by drop wise addition DI water to prepared solution, while stirring for obtaining yellow and transparent solution. Other specifications of coating process can be found on ref [26].

Plate samples ($20 \times 10 \times 2$ mm) of mild steel were used as substrates in this study. After polishing to about R_a 2 μm using an Al_2O_3 slurry, the samples were first cleaned with acetone and then ultrasonically cleaned in ethanol. Samples were dip coated in the specific solution with 0.5 mm/s dip coating rate by a dip coater rig and then pulled out from the solution by the same dip coating rate. Samples were dried in a drying rig by decreasing humidity from 85% to common laboratory atmosphere. Heat treating was done after drying in a common tube resistance furnace. The X-ray diffraction (XRD) pattern for the TiO_2 coating was obtained with X-ray diffraction system with $\text{CuK}\alpha$ radiation ($\lambda = 1.5406 \text{ \AA}$) at ranging from 10 to 60° .

The “quality characteristic” of concern is the corrosion resistance of the coatings that was assessed by tafel polarization tests carried out at 298 K using an EG&G 273A Potentiostat/galvanostat with 352 SoftCorr software. A three electrode cell with the coated samples as a working electrode, saturated calomel electrode as a reference electrode, and a platinum plate as a counter electrode was used in the tests. The ratio of the volume of 3.5 wt % NaCl solution / sample area was 200 ml/cm^2 . After the electrochemical testing system became stable (about 1 hour), scans were conducted at a rate of 0.1 mV/s. The surface morphology, uniformity, homogeneity, and its cracks for coated samples were examined by XL-30 (PHILIPS) scanning electron microscopy (SEM) and atomic force microscopy (AFM).

3. RESULTS AND DISCUSSION

Selection of Precursors

The precursors used in this study were selected due to their specific physical / chemical properties. In this work, the alkoxide precursor was selected because the

precursors containing the long-chain hydrocarbon groups comprise hydrophobic, enable better mixing of the organic functionalities at the molecular level, and promote formation of nonporous gels and the final film will reach good properties. When appropriate chemical composition and processing conditions applied, relatively dense organic-inorganic hybrid coatings can be achieved for applications including sensors, antireflection coatings, wear resistance and corrosion protection [13]. The preparation steps of this sol were as follows:

- (1) EAcAc as chelating agent was added to absolute ethanol and stirred for 10 min.
- (2) TBT precursor added to the above solution and stirred for 30 min.
- (3) The water added drop wise and carefully to the solvent and the solution stirred for 6 hours.
- (4) Prepared solution aged for 6 hours.

Coating Characterization

There are many ways to reduce the percentage of cracks on final coat performed with sol-gel method:

- (1) Usage of polymeric agents such as Polyethilen Gelicol, Poly Vinyl Alcohol, Poly Vinyl Propylene.
- (2) Usage of Acetic Acid.
- (3) Usage of ethyl Aceto Acetate and controlling the heat treatment cycle.
- (4) Usage of Hybridation process.

In first and second way, the velocity of evaporation for volatile organic agents from coating will decrease significantly. Also increasing porosity and specific area of coating will lead to significant decreasing of percentage of cracks in coating.

In third way chemical agents act like a binder and adsorb titanium compounds around their selves. Whenever the sample rinse in the solution, these compounds will bind toward the sample and hence the percentage of coated area will increase.

After evaporation of organic agents the cracks percentage will decrease. The evaporation rate and obtained stress in coating will be controlled by controlling the heat treatment conditions.

In fourth way, performed coating will expose to a heat treatment by 550°C and 10 to 30 minutes, then due to its thickness it will expose to distilled water with the temperature of 100°C and then the sample will expose to a low temperature heat treatment cycle. In this method, forming the hybrid compounds will lead to significant decrease in cracks.

The difference of thermal expansion coefficients of steel and TiO_2 nanoparticle coating is one of the main reasons of crack initiation on coating. In this article for decreasing this difference and increasing the quality of final coating, an initial coat were applied (with sol-gel method) on the surface of raw sample and it exposed to a heat treatment cycle with 550°C . This coat has a lot of cracks on it, but converts the steel substrate to a ceramic

one with the same thermal expansion coefficient with raw substrate which was shown schematically in Fig. 2. Then the second nanoparticle coat was applied on the surface of sample, However with usage of Ethyl Aceto Acetate and controlling the heat treatment parameters that have shown in Fig. 3, the evaporation rate of volatile organic agents from coating and cracks growth, were decreased significantly.

The presence of defects in final coat significantly is dependent on heat treatment cycle. Choosing critical temperatures and treatment times for heat treatment cycle is very important to obtain final coat with high quality, especially for steel in this investigation. Figure 3 schematically illustrates heat treatment cycle for achieving TiO₂ nanoparticle coating with high quality on steel substrate. The temperature changing rate on this cycle is 1°C/min. At first the coated sample heated at 40°C for 5 hours for evaporation of its moisture with minimum evaporation rate. Then temperature increased to 120°C for evaporation of remained organic agents and the sample heated for one hour in this temperature. Then the temperature increased up to 550°C and the sample remained at this temperature for 1 hour for obtaining maximum anatase phase of TiO₂ and finally the sample cooled by cooling rate of 1°C/min to ambient temperature.

The XRD spectrum indicates strong diffraction peaks of anatase phase. It shows anatase is the major phase in coating and there is not any another phase in the coating, so there is not any stress in the structure and anatase (101) and rutile (110) reflections can be seen at 25.4 and 27.4° in Fig. 4.

These results are in good compliance with thermodynamic and heat treatment properties of titanium oxide in 550°C. Anatase phase has good stability and corrosion protective characteristic on metals. In addition, quality control of anatase phase was easier compared with rutile phase at 800°C. Therefore, in this paper anatase phase was chosen as the protective coating layer.

Important factors in corrosion protection of coated samples are high quality of coating such as, thickness, crack and uniformity. Moreover, in sol-gel process, essential factors such as relevant factors of sol-gel preparation process and heat treatment rate are contributing in obtaining coatings with high quality and each of them has specific effect in coating quality. The molar ratio of precursors to other additives in solution is important. The yellow transparent sol with high stability provides the desired properties for thin film coating.

Figure 5 illustrates SEM and OM micrograph from interlayer and final TiO₂ nanoparticle coating. Quality and percentage of cracks for interlayer coating can be seen in this figure. Interlayer coat due to its high difference in thermal expansion coefficient with raw substrate has a lot of defects. These cracks and defects are beneficial for adherence of final coat because the adherence nature in sol-gel method is physical, not chemical.

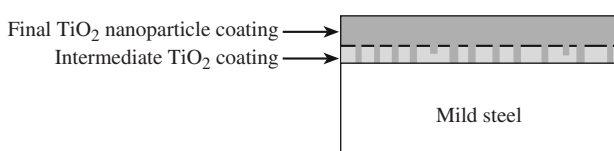


Fig. 2. Intermediate layer and final layer of TiO₂ nanoparticle coating on mild steel.

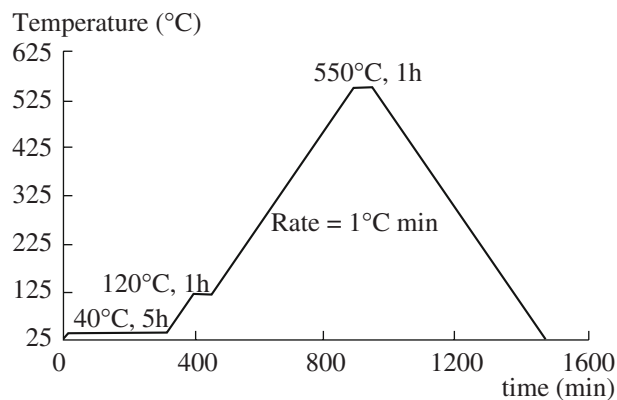


Fig. 3. Heat treatment cycle of coating process.

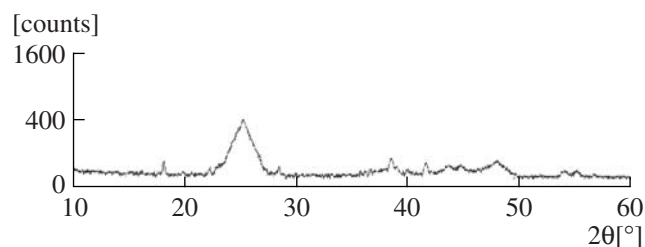


Fig. 4. XRD diffraction curve of TiO₂ coating on mild steel.

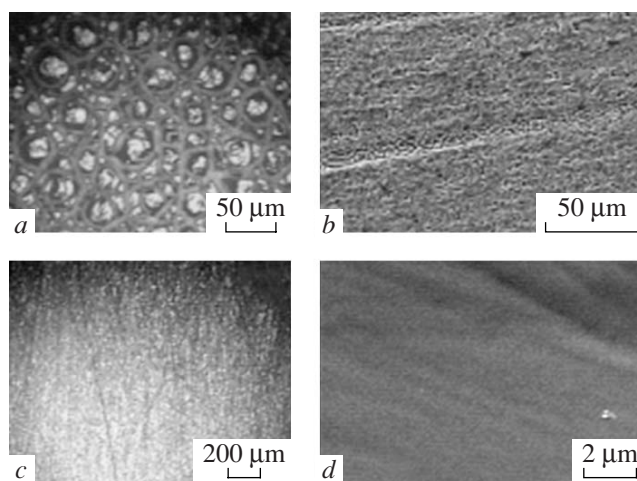


Fig. 5. (a) OM micrograph of sol-gel intermediate TiO₂ coated steel surface. (b) SEM micrograph of sol-gel intermediate TiO₂ coated steel surface. (c) OM micrograph of sol-gel final TiO₂ coated steel surface. (d) Micrograph of sol-gel final TiO₂ coated steel surface.

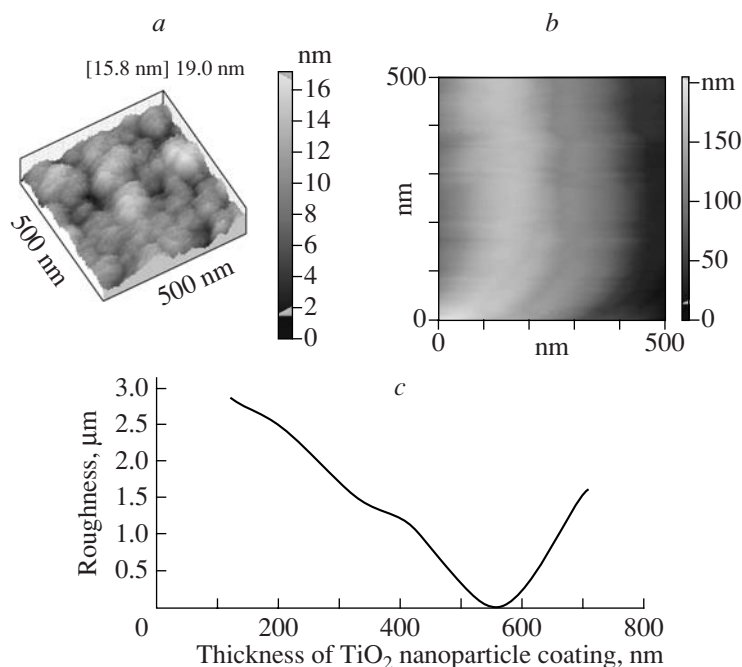


Fig. 6. AFM nanograph of TiO₂ nanoparticle coating on mild steel by sol-gel method: (a) morphology of surface (b) cross section, (c) relationship between roughness of TiO₂ nanoparticle coating and its thickness obtained by AFM.

It also exhibits a uniform and complete coating with no cracking and results in corrosion resistance improvement of metals. Homogeneous, crack-free, optically transparent and uniform coatings (as shown in Fig. 5) with thicknesses on the order of 500–700 nm were produced in this investigation.

AFM figures from performed coats indicate their homogeneity and roughness. Stainless steels due to Cr₂O₃ presence on their surface (and their low difference with TiO₂ thermal expansion coefficient) are more suitable than mild steel for substrate of sol-gel method. In this article by performing an interlayer on the surface of sample, the difference of thermal expansion coefficients between substrate and coat has been reduced.

Final coating was studied with AFM and its roughness was in nanometric scale. Figure 6 illustrates AFM result of final coat. The TiO₂ nanoparticle sizes were about 40 to 60 nm obtained from XRD and AFM.

The thickness of performed TiO₂ nanoparticle coating on steel substrate has been calculated by AFM topography illustrated in Fig. 6 and by DualScope software.

The calculation of the corrosion resistance of samples is based on the corrosion potential, the corrosion current density, and the anodic/cathodic Tafel slopes (β_a and β_c) which were derived from the measured polarization curves. Based on the approximately linear polarization at the corrosion potential (E_{corr}), the value of corrosion resistance (R_p) was determined from the relationship:

$$R_p = \frac{\beta_a \beta_c}{2.3 i_{\text{corr}} (\beta_a + \beta_c)} \quad (1)$$

where i_{corr} is the corrosion current density.

The results of the Tafel polarization corrosion tests for the different coatings on mild steel are given in Table 1, which also includes data for the substrate for the purpose of comparison. Figure 7 shows Tafel polarization curves for six samples in 3.5 wt % NaCl solution. The electrochemical parameters obtained from Tafel curves are given in Table 1. From anodic current densities (i_{corr}) and corrosion resistances (R_{corr}), it is evident that coated mild steel has good tendency of corrosion resistance behaviour. Applied TiO₂ nanoparticle coating decreases i_{corr} by nearly 100 times which is apparent that poor corrosion resistance of mild steel in

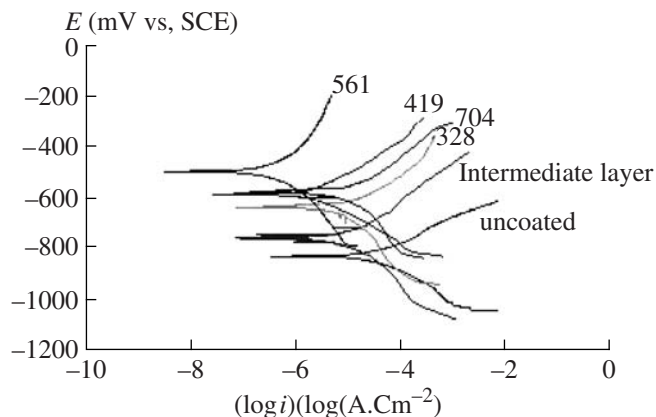


Fig. 7. Tafel polarization curves of the substrate mild steel and TiO₂ nanoparticle coating.

Table 1. Different electrochemical parameters obtained by Tafel extrapolation and impedance analysis

Thickness of TiO ₂ coating, nm	OCP, mV	i_{corr} , $\mu\text{A}/\text{cm}^2$	β_a , mV/decade	β_c , mV/decade	R_p
Mild steel	-824.9	18.621	137.2	168.9	1767.623
Intermediate layer 193	-754	8.3652	154.8	294.7	5274.936
328	-632.7	7.7096	149.2	268.6	5409.371
419	-583	2.4831	198.9	223.8	18439.136
561	-501	0.17378	234.8	321.1	339323.6229
704	-570	2.1668	118.5	291.4	16903.759

Note: R_p (Corrosion resistance) (Ohm C m^2).

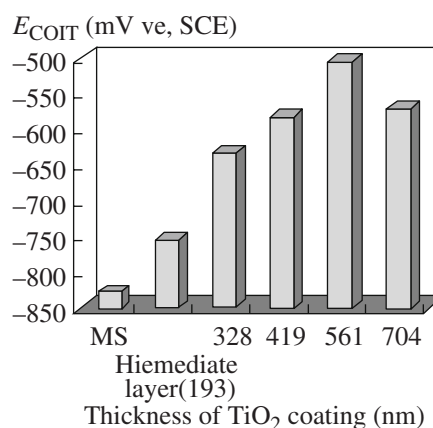
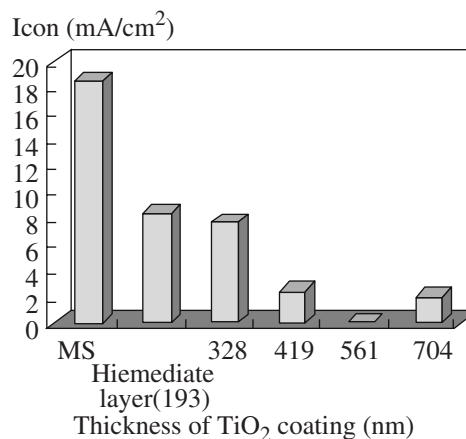
3.5 wt % NaCl have intensively promoted due to formation of stable and inactive TiO₂ coating.

Figure 8 shows relationship between thicknesses of TiO₂ nanoparticle coating and its corrosion potential. This figure indicates that open circuit potential of TiO₂ nanoparticle coating is more noble than bare steel. The TiO₂ nanoparticle coating with thickness of 561 nm has the most noble open circuit potential. Changing the kinetics of cathodic and anodic reactions will lead to different open circuit potentials. TiO₂ nanoparticle coating changes the slope of anodic and cathodic branches of Tafel curve and as its result the kinetic of cathodic and anodic reaction will change, so OCP of the coated sample will shift to positive direction. Cathodic polarization will occur immediately when TiO₂ nanoparticle coating expose in 3.5 wt % NaCl solution. Also anodic reaction will change and the corrosion rate or i_{corr} will decrease due to applied TiO₂ nanoparticle coating on steel. Cathodic reaction is water reduction but anodic reaction is related to TiO₂ nanoparticle coating for coated samples and it is related to steel for uncoated samples. TiO₂ nanoparticles increase contact between coating and NaCl solution, so the intensity of anodic reaction will increase. This aspect has two sides, first, nanoparticles will increase intensity of anodic and cathodic reactions, and second, nanoparticles will increase homogeneity and uniformity of coating and also will decrease defects of coating. Therefore nanoparticles control defects on molecule's level and will lead to high increasing corrosion protection properties. Presence of nanodefects in the nanoparticle coating probably will isolate anodic reactions as a filter and also decrease intensity of reactions.

Figure 9 shows relationship between thickness of TiO₂ nanoparticle coating and corrosion current (i_{corr}). In this figure i_{corr} has been decreased about 100 times compared with bare steel when TiO₂ nanoparticle coating applied on steel. The thickness of this coating is 561 nm.

This figure shows that i_{corr} decreases when the thickness of TiO₂ nanoparticle coating increases. It is probably related to eliminating or decreasing defects of first layer of TiO₂ nanoparticle coating by upper layers. Increasing thickness of coating will lead to decreasing of electron transition and rate of electrochemical reactions.

Adhesion of coating will decrease when TiO₂ nanoparticle coating grow more than 561nm. Adherence of coating in sol gel process has physical nature and depends on defects of surface, therefore adherence of coating decrease when thickness of coating grow up and also brittle ability of TiO₂ nanoparticle coating will increase. Decreasing adherence of coating to bare steel and generation stress in TiO₂ nanoparticle coating are

**Fig. 8.** E_{corr} vs. Thickness of TiO₂ coating on mild steel.**Fig. 9.** Relativity between thickness of TiO₂ coating on mild steel and corrosion current density.

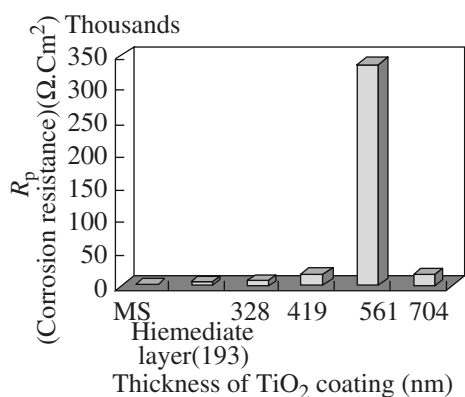


Fig. 10. Relativity between thickness of TiO₂ coating on mild steel and corrosion resistance.

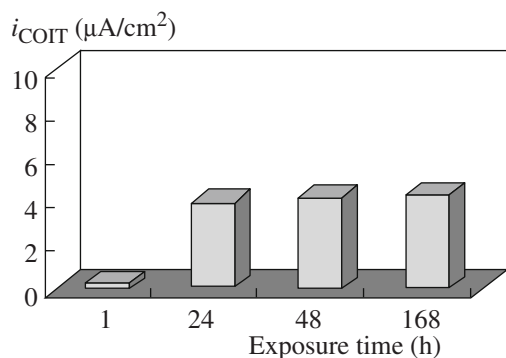


Fig. 12. Relativity between exposure time of TiO₂ nanoparticle coating in 3.5 wt % NaCl solution and corrosion current density.

results of pressure made by exiting volatile organic compositions during heat treatment. Increasing the stress from critical amount will produce cracks and defects in final coating. Therefore presence of defects and cracks in coating will increase corrosion rate of coating. This result has been seen for coating with thickness of 704 nm in Fig. 8. Corrosion resistance (R_p) as a result of corrosion current density (i_{corr}) can be seen schematically in Fig.10.

Figure 11 shows Tafel polarizations of TiO₂ nanoparticle coating which was performed at 1, 24, 48 and

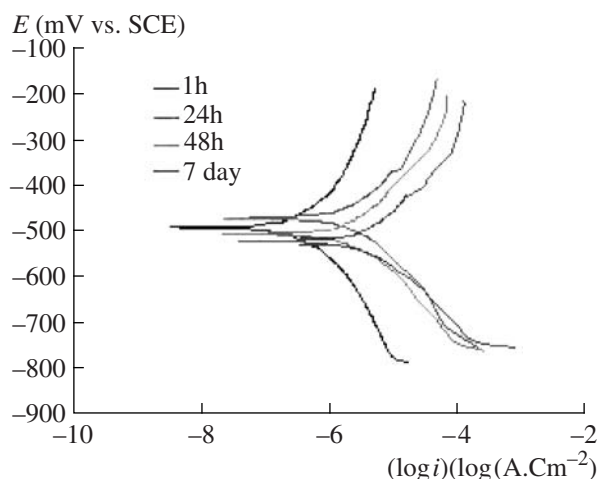


Fig. 11. Tafel polarization curves of TiO₂ nanoparticle coating at different exposure times.

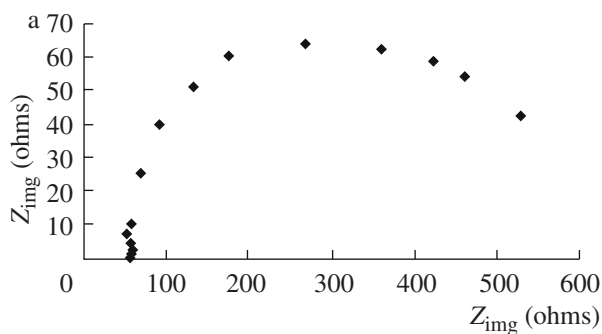


Fig. 13. Typical Nyquist diagram (a) mild steel (b) TiO₂ nanoparticle coating.

168 hours of immersion time. The details of this figure summarized in Table 2 which were used for comparing corrosion properties of coating at different immersion times. According to Fig. 12, after 24 hours of immersion, corrosion current density will remain constant that indicates good stability of this coating.

Increasing of R (coating resistance) in Fig. 13 confirms the improvement of corrosion resistance of samples by this coating process. The mechanism of corrosion resistance improvement of these coatings is acting

Table 2. Different electrochemical parameters obtained by Tafel extrapolation of TiO₂ nanoparticle coating with thickness of 561 nm for different exposure times on to 3.5 wt % NaCl solution

Time, h	OCP, mV	I_{corr} , A/cm ²	β_a , mV/decade	β_c , mV/decade	R_p , KOhm Cm ²
1	-501	1.7378E-7	234.8	321.1	33932.362
24	-475	3.9652E-6	191.6	301.9	11674.532
48	-513	4.1863E-6	205.4	316.4	11313.711
168	-531	4.3624E-6	200.8	287.5	6622.028

Note: R_p —Corrosion resistance, KOhm Cm².

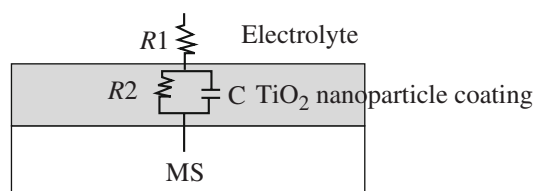


Fig. 14. Equivalent electrical circuit (EES) of TiO₂ nanoparticle coatings

of these coatings like capacitive coating and delaying anodic reactions.

Equivalent electrical circuit (EES) of these coatings has been illustrated in Fig. 14. In this figure R_2 and C are related to perfect TiO₂ nanoparticle coating over mild steel and R_1 is for resistance of solution in contact by coating. Capacitance is related to coating thickness and the percentage of defects on it.

CONCLUSIONS

TiO₂ nanoparticle coating has been performed on mild steel by sol-gel method. TiO₂ nanoparticle coating with properties such as homogeneity and crack-free increase E_{corr} and cathodic slope and result in highly improvement corrosion resistance of mild steel in 3.5 wt % NaCl solution. A uniform and complete TiO₂ nanoparticle coating without any cracks improve corrosion resistance of metals, such as stainless steel, aluminum and titanium, as a barrier layer.

Achieving high quality coating is related to different parameters of solution and heat treatment. So the temperature of 550°C choose to obtain the best coating quality in high temperatures. Anatase was determined by heat treatment at 550°C on the surface of sample. TiO₂ nanoparticle coating with thickness of 561 nm will shift the open circuit potential about 320 mV. Increasing the coating thickness up to 561nm will improve corrosion properties of coated sample. Corrosion resistance of mild steel by performing this coating will improve about 190 times better than raw substrate. Increasing the coating thickness more than 561 nm will decrease physical and corrosion properties of coated sample than coated samples with coating thickness less than 561 nm. TiO₂ nanoparticle coating with capacitive properties will decrease corrosion current density of mild steel.

ACKNOWLEDGMENTS

The authors would like to express their thanks to the nanoscience and nanotechnology research organization and also National Iranian Gas Company.

REFERENCES

- Bonini, N., Carotta, M.C., Chiorini, A., et al., *Sens. Actuators, Ser. B: Chem.*, 2000, vol. 68, p. 274.
- Ivanova, T., Harizanova, A., Surtchev, M., and Nenova, Z., *Sol. Energy Mater. Sol. Cells*, 2003, vol. 76, p. 591.
- Perera, V.P.S., Jayaweera, P.V.V., Pitigala, P.K.D.D.P., et al., *Synth. Met.*, 2004, vol. 143, p. 283.
- Keshmiri, M., Mohseni, M., and Troczynski, T., *Appl. Catal., Ser. B: Environ.*, 2004, vol. 53, p. 209.
- Mao, D., Lu, G., and Chen, Q., *Appl. Catal., Ser. A: Gen.*, 2004, vol. 263, p. 83.
- Huang, S.Y., Kavan, L., Exnar, I., and Gratzel, M., *J. Electrochem. Soc.*, 1995, vol. 142, p. L142.
- Aliev, A.E. and Shin, H.W., *Displays*, 2002, vol. 32, p. 239.
- Fretwell, R. and Douglas, P., *J. Photochem. Photobiol., Ser. A: Chem.*, 2001, vol. 143, p. 229.
- Tai, W.P. and Oh, J.H., *Sens. Actuators, Ser. B: Chem.*, 2002, vol. 85, p. 154.
- Karunakaran, B., Uthirakumar, P., Chung, S.J., et al., *Materials Characterization*, 2007, vol. 58, p. 680.
- Shen, G.X., Chen, Y.C., and Lin, C.J., *Thin. Solid. Films*, 2005, vol. 489, p. 130.
- Sberveglieri, G., Depero, L.E., Ferroni, M., et al., *Adv. Mater.*, 1996, vol. 8, p. 334.
- Bally, A.R., Korobeinikova, E.N., Schmid, P.E., et al., *J. Phys., Ser. D: Appl. Phys.*, 1998, vol. 31, p. 149.
- Carotta, M.C., Ferroni, M., Guidi, V., and Martinelli, G., *Adv. Mater.*, 1999, vol. 11, p. 943.
- Chow, L.L.W., Yuen, M.M.F., Chan, P.C.H., and Cheung A.T., *Sens. Actuators, Ser. B*, 2001, vol. 76, p. 310.
- Tuan, A., Yoon, M., Medvedev, V., et al., *Thin. Solid. Films*, 2000, vol. 377/378, p. 766.
- Kang, B.C., Lee, S.B., and Boo, J.H., *Surf. Coat. Technol.*, 2000, vol. 131, p. 88.
- Liu, X., Yin, J., Liu, Z.G., et al., *Appl. Surf. Sci.*, 2001, vol. 174, p. 35.
- Ong, C.K. and Wang, S.J., *Appl. Surf. Sci.*, 2001, vol. 185, p. 47.
- Tang, H., Prasad, K., Sanjines, R., and Levy, F., *Sens. Actuators, Ser. B*, 1995, vol. 26/27, p. 71.
- Garzella, C., Comini, E., Tempesti, E., et al., *Sens. Actuators, Ser. B*, 2000, vol. 68, p. 189.
- Brinker, C.J. and Schere, G.W., *Sol-Gel Science*, N.Y.: Academic Press, 1990.
- Gluszek, J., Jedrkowiak, J., and Markowski, J., *J. Masalski. Biomaterials*, 1990, vol. 11, p. 330.
- Hawthorne, H.M., Neville, A., Troczynski, T., et al., *Surf. Coat. Technol.*, 2004, vol. 176, p. 243.
- Ruhi, G., Modi, O.P., Singh, I.B., et al., *Surface and Coatings Technol.*, 2006, vol. 201, p. 1866.
- Shanaghi, A., Sabour Rouhaghdam, A., Shahrabi, T., and Aliofkhaezai, M., *Materials Sci.* (in press).